PERGAMON

Quaternary Science Reviews 22 (2003) 2311–2326

QSR

Persistent millennial-scale climatic variability over the past 25,000 years in Southern Africa

Karin Holmgren[a,*], Julia A. Lee-Thorp[b], Gordon R.J. Cooper[c], Katarina Lundblad[a], Timothy C. Partridge[d], Louis Scott[e], Riashna Sithaldeen[b], A. Siep Talma[f], Peter D. Tyson[d]

[a] *Department of Physical Geography and Quaternary Geology, Stockholm University, S-106 91 Stockholm, Sweden*
[b] *Department of Archaeology, University of Cape Town, Private Bag, Rondebosch, Cape Town 7701, South Africa*
[c] *School of Geosciences, University of the Witwatersrand, PO Wits, 2050, South Africa*
[d] *Climatology Research Group, University of the Witwatersrand, PO Wits, 2050, South Africa*
[e] *Department of Plant Sciences, University of the Free State, Bloemfontein 9300, South Africa*
[f] *Quaternary Dating Research Unit, CSIR, PO Box 395, Pretoria 0001, South Africa*

Received 23 December 2002; accepted 8 June 2003

Abstract

Data from stalagmites in the Makapansgat Valley, South Africa, document regional climatic change in southern Africa in the Late Pleistocene and Holocene. A new TIMS U-series dated stalagmite indicates speleothem growth from 24.4 to 12.7 ka and from 10.2 to 0 ka, interrupted by a 2.5 ka hiatus. High-resolution oxygen and carbon stable isotope data suggest that postglacial warming was first initiated ~17 ka, was interrupted by cooling, probably associated with the Antarctic Cold Reversal, and was followed by strong warming after 13.5 ka. The Early Holocene experienced warm, evaporative conditions with fewer C_4 grasses. Cooling is evident from ~6 to 2.5 ka, followed by warming between 1.5 and 2.5 ka and briefly at ~AD 1200. Maximum Holocene cooling occurred at AD 1700. The new stalagmite largely confirms results from shorter Holocene stalagmites reported earlier. The strongest variability superimposed on more general trends has a quasi-periodicity between 2.5 and 4.0 ka. Also present are weaker ~1.0 ka and ~100-year oscillations, the latter probably solar induced. Given similarities to the Antarctic records, the proximate driving force producing millennial- and centennial-scale changes in the Makapansgat record is postulated to be atmospheric circulation changes associated with change in the Southern Hemisphere circumpolar westerly wind vortex.

1. Introduction

Until recently no continuous, multi-millennial, high-resolution terrestrial proxy climate records existed for southern Africa. In 1999 the first, derived from stable isotopes from two stalagmites taken from Cold Air Cave in the Makapansgat valley in north-eastern South Africa (Fig. 1), provided a 3.5 ka record of $\delta^{18}O$ and $\delta^{13}C$ variability at a resolution of about 10 years (Holmgren et al., 1999). The record was later extended to 6.6 ka (Lee-Thorp et al., 2001). In order to verify the results obtained from one continuous (T7) and one semi-continuous specimen (T5), a third stalagmite (T8), taken about 10 m from T7, has been analysed and provides a high-resolution record back to 24.4 ka. In this paper, the comparability of records is examined, the chronicle of climatic change and variability contained in T8 is considered for the past 24.4 ka, and the results are compared with those from other sites, primarily in the Southern Hemisphere.

The availability of highly resolved and reproducible records from the Makapansgat Valley, with excellent time control during the Holocene in particular, permits comparisons with similarly well-dated records elsewhere and, in some cases, allows the problem of leads and lags to be addressed. A great deal of argument has surrounded the question of whether climate shifts within the Northern and Southern Hemispheres are asynchronous or not, but data series, particularly terrestrial ones, with the requisite resolution to resolve the synchroneity problem are rare. A possibility raised by the stalagmite evidence presented here is that some events may be globally synchronous while others may not.

*Corresponding author. Tel.: +46-8-6747157; fax: +46-8-164818.
E-mail address: karin.holmgren@natgeo.su.se (K. Holmgren).

0277-3791/$ - see front matter © 2003 Elsevier Ltd. All rights reserved.
doi:10.1016/S0277-3791(03)00204-X

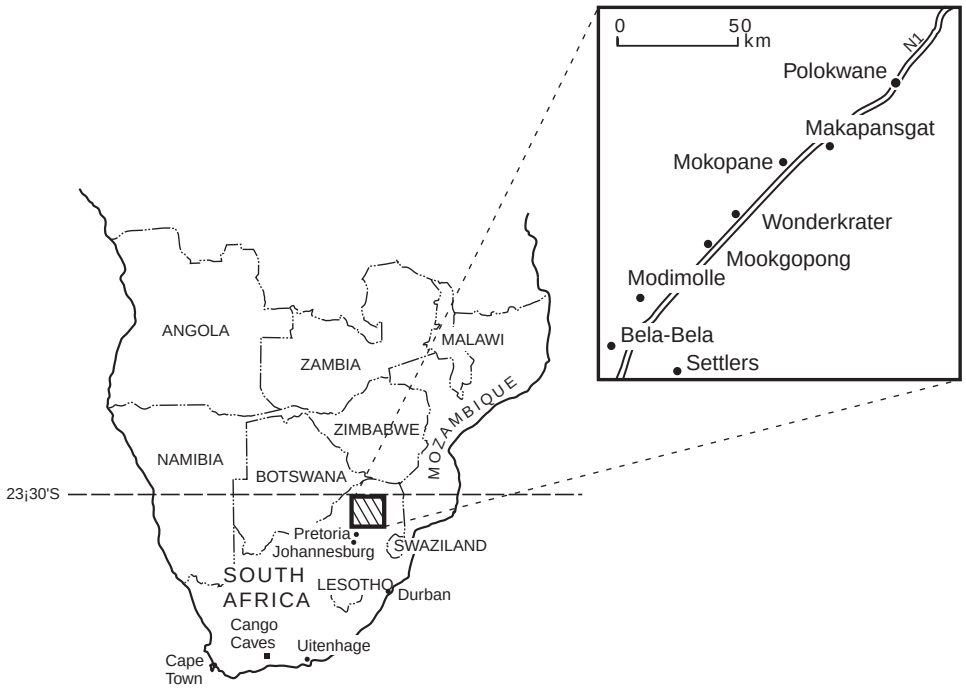

Fig. 1. Location map showing places mentioned in the text. Polokwane was formerly known as Pietersburg, Mokopane as Potgietersrus, Modimolle as Nylstroom, Mookgopong as Naboomspruit, and Bela Bela as Warmbaths. Pretoria per se has retained its name, whereas Greater Pretoria is now known as Tshwane.

2. Methods and data

Cold Air Cave is situated in the Makapansgat Valley (24°1′S, 29°11′E) in the summer rainfall region of South Africa (Fig. 1), where over 90% of the mean annual rainfall (521 mm) at the nearest major weather station in Polokwane (formerly Pietersburg) is experienced in summer (October–April) (Schulze, 1984). The southern Indian Ocean is presently the major atmospheric moisture source area. The climate is mild with a mean mid-summer daily maximum temperature of 27°C, a mean mid-winter daily minimum temperature of 2.4°C, and a diurnal range of 11.3°C and 17.1°C in mid-summer and mid-winter, respectively. The valley is characterised by a vegetation of North-Eastern Mountain Sourveld type, transitional to Sourish Mixed Bushveld (Acocks, 1953) or Mixed Savanna (Scholes, 1997), which includes a large C_4 grass component.

Cold Air Cave is located in a dolomitic karst system. The sampled stalagmites were located some 100 m from the narrow entrance, and 10 m apart beneath separate fissures within the dolomite roof of the cave. Each fissure is marked by a line of small stalactites, and acts as a separate conduit from a small surface catchment above the cave to the growing speleothems below. The cave climate close to the stalagmites has been monitored semi-continuously over 2 years as part of an ongoing project. Relative humidity, temperature and shifts in the amounts of dripwater have been recorded, and dripwater samples were collected for analysis of $^{18}O/^{16}O$ ratios. In addition, groundwater samples of recent and fossil ages were obtained 120–150 km south-west of Makapansgat from hot springs at Bela Bela (formerly Warmbaths) and from boreholes near the Settlers village 30 km east of Bela Bela (Fig. 1). The samples were analysed for $^{18}O/^{16}O$ composition in order to establish general trends in the composition of past precipitation and of drip water feeding the stalagmites. Ages were calculated from the ^{14}C content of the groundwater using an initial content of 0.85 to account for dead carbon dilution and calibrated with INTCAL98 (Stuiver et al., 1998), extended with a calibration curve derived from a stalagmite from Cango Cave in the southern coastal region of South Africa (Vogel and Kronfeld, 1997).

Thirty 2–3 g samples were taken along the growth axis of the 1.4-m T8 stalagmite and dated by high-precision thermal ionisation mass spectrometry (TIMS) using standard procedures (Jaffey et al., 1971; Cheng et al., 2000). In this case dating by the $^{230}Th/^{234}U$ method yields ages in calendar years before AD 2000. Small (<0.1 mg) samples were drilled for stable oxygen and carbon isotopic analysis at approximately 1-mm intervals along the stalagmite growth axis, using a 0.6-mm diamond-tipped drill. All stable isotope analyses on water and carbonate were performed using standard equilibrium techniques on a Finnigan Mat 252 mass spectrometer. Measurements were calibrated using NBS standards 18 and 19 and inter-laboratory standards Carrara Z and Lincoln Limestone. Isotope ratios are

expressed in the δ notation relative to PDB for carbonate and SMOW for water, in parts per mil. (‰).[1] Precision as determined on multiple determinations of carbonate standards is better than 0.1 per mil. for both $\delta^{13}C$ and $\delta^{18}O$.

The analysis of patterns of variability was undertaken using wavelet transform analysis. This involves a transform from a one-dimensional time series (or frequency spectrum) to a two-dimensional time–frequency image (Lau and Weng, 1995; Torrence and Compo, 1998). A wavelet analysis will thus clearly show frequency and amplitude modulation of climatic oscillations over time. Several choices of wavelet functions exist. We have chosen to use the Morlet wavelet and continuous wavelet transform, rather than the discrete wavelet transform, since the greater number of scales at which continuous wavelet transform can be calculated (for a given data set) aids in the visual interpretation of the results. The real wavelet function was used (instead of the complex wavelet function), which resulted in a continuous wavelet transform whose coefficients are contoured as a function of time and frequency in the figures (following an adjustment to convert scale to the centre frequency of the wavelet). Instead of establishing the temporal continuity of the signal by plotting the absolute value of the continuous wavelet transform as some do, contouring of the signed coefficients themselves was employed here to establish the phase relationships between the different frequency components. This facilitates a clearer interpretation of the data and provides a useful distinction between positive- and negative-amplitude peaks. A persistent oscillation appears as an unbroken ridge of positive values in the standard presentation, but as a series of positive and negative values in the presentation used here, with the instantaneous sign of the oscillation indicated by the sign of the wavelet transform. In order to overcome the problem of irregular time intervals between data points in the stalagmite record, linear interpolation was used to provide regularly spaced data. This has little or no effect on the frequency of any oscillations that may be present in the data, but has the effect of diminishing their amplitude and rendering the wavelet analyses slightly more conservative. Whether oscillations should be tested for statistical significance is a moot point (Nicholls, 2000), especially in the case of exploratory studies (Flueck and Brown, 1993). Such is the case here and it can be argued that null hypothesis significance testing may actually be misleading (Cohen, 1990; von Storch and Zwiers, 1999), especially when the total data population and not just samples of it are being considered (Nicholls, 2000).

[1] $\delta^{18}O_{PDB,\ SMOW} = (R_{sample}/R_{ref} - 1) \times 1000$, where $R = {}^{18}O/{}^{16}O$. $\delta d^{13}C_{PDB,\ SMOW} = (R_{sample}/R_{ref} - 1) \times 1000$, where $R = {}^{13}C/{}^{12}C$.

3. Results

3.1. Groundwater

The ground water isotope data form three groups: a recent group ($^{14}C > 100$ pmc; age < 50 years) with $\delta^{18}O$ from –1.5‰ to –2.9‰, a Holocene group (^{14}C 40–100 pmc; age 50–5000 years) with $\delta^{18}O$ from –3.7‰ to –4.4‰ and a Late Pleistocene group (older than 14 ka) with $\delta^{18}O$ from –4.4‰ to –5.2‰ (Fig. 2a). The high and variable ^{18}O content of the recent group can be explained by the fact that these water samples are derived from urban areas or recently developed agricultural lands where there is much opportunity for evaporation enrichment. The ^{18}O content of the Holocene group is closer to that of rainfall of the region (sampled at Pretoria, 120 km south of Bela Bela and averaging –3.7‰ for 1958–1985 (IAEA, 1992)) and is assumed to represent natural recharge processes comparable to that of the Late Pleistocene group. On this basis a local groundwater $\delta^{18}O$ curve was constructed, comprising values between –3.6‰ and –4.4‰ for the Holocene and between –4.4‰ and –5.2‰ for the Late Pleistocene (Fig. 2b). The general pattern of ^{18}O between Late Pleistocene and Holocene is similar to that obtained from artesian water in Uitenhage (Heaton

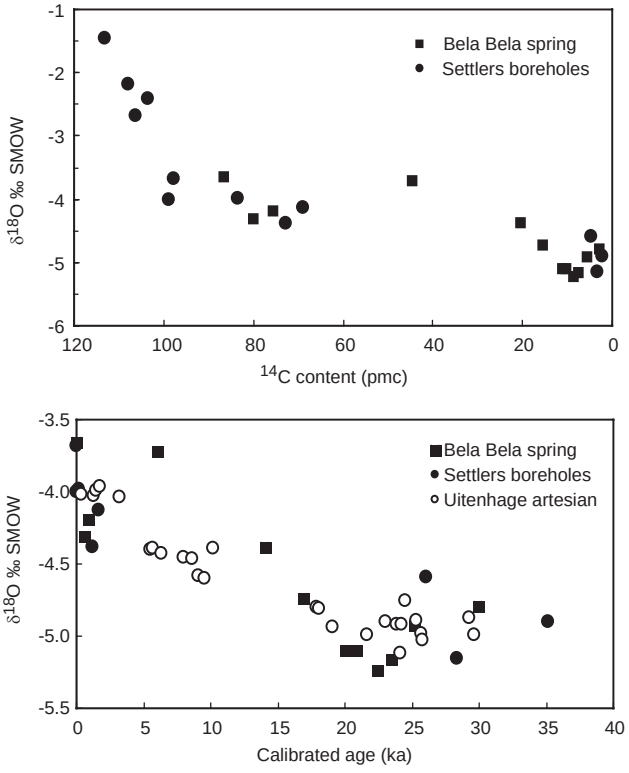

Fig. 2. $\delta^{18}O$ content (in ‰ SMOW) of groundwater samples from Bela Bela hot springs (Verhagen, 1980) and Settlers boreholes as a function of radiocarbon content (a) and against calibrated ages (b). The $\delta^{18}O$ composition of artesian water from Uitenhage (Heaton et al., 1986) is shown for comparison.

et al., 1986) (Fig. 2b), which is about 1000 km to the south of Makapansgat along the Eastern Cape coast (Fig. 1).

3.2. Cave environment

Preliminary results of the climate monitoring study show that relative humidity remains at ~100% in Cold Air Cave throughout the year, temperature remains between 18.5°C and 19.0°C, and that seepage water responds rapidly (within 6 weeks) to onset of the rainy season. Dripwater amount declines markedly in the dry (winter) season. Isotopic values of dripwater samples near the stalagmite locations have a mean value of about –4‰, remaining relatively stable throughout the year in spite of the large seasonal changes in dripwater quantity. Indications are that values may be slightly higher (by up to 0.5‰) at the end of the dry winter season. It appears that the isotopic composition of the dripwater remains consistent except for brief changes after extreme precipitation events. A major flood event in February 2000 resulted in a transient change of −1.0‰ at the next collection.

3.3. Age of stalagmite T8

Results of the $^{230}Th/^{234}U$ age determinations are presented in Table 1. No samples display sufficient ^{232}Th contamination ($^{230}Th/^{232}Th$ <20) to affect the age determinations. Stalagmite growth occurred over the past 24.4 ka. For the period 0–12.7 ka, T8 is composed of aragonite, like the previously analysed T5 and T7 stalagmites from the same cave. Rapid growth rate (11 mm/100 years), high chemical yields and well-resolved energy spectra resulted in precise age determinations for this period. An age model (Fig. 3) was produced by linear interpolation between dated intervals for the period 0–10.2 ka. A large age gap between two closely spaced high-precision dated samples indicates the presence of a 2.5 ka hiatus at 10.2–12.7 ka. Between 12.7 and 24.4 ka the stalagmite is composed of calcite and dating precision is poorer owing to the low U content and slow growth rate (2 mm/100 years). For this section the age model was derived by linear regression over the whole period (Fig. 3). Excellent dating precision of ±6–160 years was achieved for the period 0–12.7 ka; prior to this, precision declines from about 500 years at 13 ka to about 3000 years at 24.4 ka.

Table 1
TIMS uranium series dates of stalagmite T8, Cold Air Cave, Makapansgat Valley. Ratios are activity ratios expressed with 2σ (numbers in brackets give the statistical uncertainty of the last significant digit)

Sample	mm	U (ppm)	$^{234}U/^{238}U$	$^{230}Th/^{234}U$	$^{230}Th/^{232}Th$	Age (year)
T8-21	21	1.502 (5)	11.78 (6)	0.00150 (3)	269±5	113±6
T8-20	43	0.942 (2)	8.72 (3)	0.0034 (1)	531±20	321±28
T8-19	62	0.854 (4)	8.95 (5)	0.00429 (10)	141±2	418±14
T8-18	101	0.911 (2)	9.66 (3)	0.00646 (4)	740±5	654±9
T8-17	117	1.095 (3)	9.61 (4)	0.00728 (10)	690±10	744±24
T8-16	181	1.026 (3)	9.57 (7)	0.01337 (10)	814±4	1411±17
T8-15	215	0.924 (3)	9.75 (5)	0.01549 (10)	959±15	1644±14
T8-14	234	1.040 (4)	10.36 (6)	0.01670 (10)	1054±5	1778±22
T8-13	258	0.909 (5)	9.9 (1)	0.01772 (20)	297±2	1890±37
T8-12	276.5	0.990 (5)	9.24 (8)	0.01903 (30)	1450±26	2034±73
T8-11	296	0.927 (2)	9.09 (4)	0.01986 (30)	859±14	2170±71
T8-29	363	1.475 (5)	10.06 (5)	0.02637 (10)	1543±8	2845±31
T8-08	502	0.968 (2)	10.57 (3)	0.03236 (30)	2624±27	3549±57
T8-07	602	1.474 (8)	10.48 (9)	0.04277 (30)	8334±56	4674±74
T8-28	650.5	2.258 (9)	10.49 (7)	0.04655 (30)	10,421±50	5100±59
T8-06	812.5	2.246 (4)	9.73 (3)	0.060758 (30)	12,377±65	6748±31
T8-27	887	2.56 (1)	6.78 (5)	0.06819 (40)	11,717±46	7558±88
T8-05	977	1.95 (1)	6.09 (5)	0.07649 (60)	14,903±127	8556±145
T8-26	1039	1.3298 (2)	6.17 (1)	0.08396 (20)	5276±28	9378±56
T8-04	1131.5	0.863 (4)	6.81 (5)	0.09016 (70)	389±3	10,141±160
T8-31	1135.5	1.2349 (7)	7.70 (8)	0.11182 (70)	8867±52	12,687±160
T8-03	1160	0.03703 (6)	7.39 (4)	0.10849 (580)	250±13	12,280±1366
T8-32	1166.5	0.03969 (9)	7.21 (4)	0.12680 (130)	3922±177	14,474±331
T8-25	1175.5	0.0380 (1)	7.06 (4)	0.11608 (250)	116±2	13,145±584
T8-2b	1191	0.0983 (2)	7.59 (4)	0.11092 (180)	199±3	12,580±422
T8-02	1205.5	0.02220 (6)	6.99 (6)	0.14583 (100)	394±3	16,726±243
T8-24	1217.5	0.02551 (4)	7.46 (4)	0.13061 (510)	255±10	14,880±1225
T8-23	1289.5	0.0426 (2)	8.05 (5)	0.16194 (300)	303±6	18,691±735
T8-34	1326.5	0.0274 (3)	8.27 (12)	0.21611 (330)	1087±13	25,571±854
T8-22	1360	0.0250 (2)	8.9 (1)	0.20082 (370)	242±4	23,554±930
T8-01	1384.5	0.02254 (2)	7.56 (2)	0.18638 (300)	109±2	21,777±759

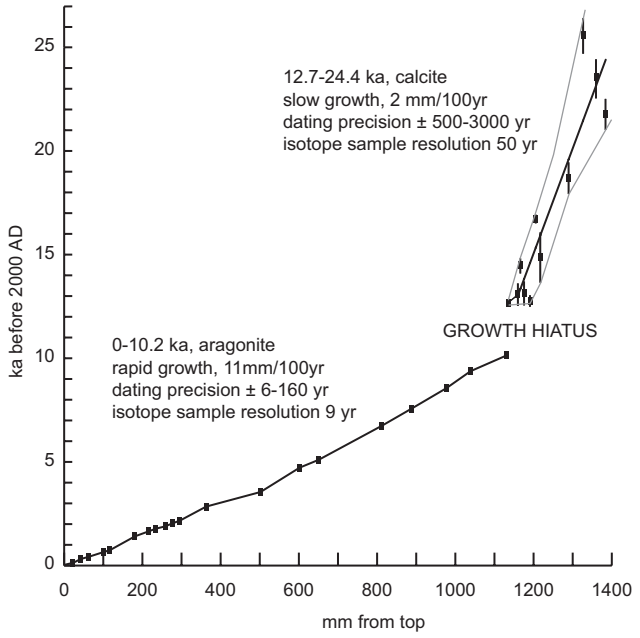

Fig. 3. Absolute ages with errors (2σ) and interpolated growth for the T8 stalagmite from Cold Air Cave, Makapansgat Valley.

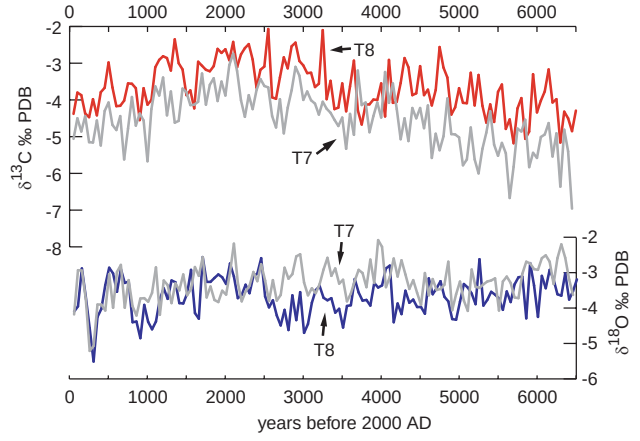

Fig. 4. Comparison of 6.6 ka of Makapansgat $\delta^{18}O$ and $\delta^{13}C$ records for stalagmites T7 (Lee-Thorp et al., 2001) and T8 resolved at 50-year intervals.

3.4. Stalagmite isotopic composition

The above age model allows an average isotope sample resolution of 9 years for the period 0–10.2 ka and of 50 years for 12.7–24.4 ka. The T7 and T8 $\delta^{18}O$ and $\delta^{13}C$ records can be compared where they overlap for the past 6.5 ka (Fig. 4). The two records compare well for both $\delta^{18}O$ and $\delta^{13}C$; the frequency of occurrence of peaks or troughs of opposite sign in the two data series is less than 5%. It may be concluded that the stalagmite-derived stable isotope proxies provide a robust signal of local climatic and environmental change. Caution must be exercised, however, since discrepancies do occur, e.g. in the case of $\delta^{18}O$ at 2.6–3.5 ka. These may be a result of small differences in the age models leading to differences in apparent ages for given periods, or may reflect real differences between the records due to local variations. The full 0–24.4 ka $\delta^{18}O$ and $\delta^{13}C$ records for T8, plotted at 50-year intervals, are given in Fig. 5. Because aragonite and calcite have different fractionation factors, in order to be comparable with the calcite section (12.7–24.4 ka) values for the aragonite section in the stalagmite (0–12.7 ka) have been corrected by −0.6‰ for $\delta^{18}O$ and by −1.8‰ for $\delta^{13}C$ (Tarutani et al., 1969; Grossman and Ku, 1986). Since the $\delta^{18}O$ signal is derived from rainfall and ultimately oceanic source, the $\delta^{18}O$ record is further corrected for global ice volume following Guilderson et al. (2001), in order to ensure comparability across the entire period.

3.5. Variability

Wavelet analysis of both $\delta^{18}O$ and $\delta^{13}C$ variations in the 24.4 ka Makapansgat record reveals complex changes in climatic variability. The general pattern of changes given by the T7 and T8 $\delta^{18}O$ records for the 6.5 ka overlap period is similar, though not identical (Fig. 6). Some of the distinctions are likely influenced by the different lengths of the two records. In the case of the T8 $\delta^{18}O$ record for the 24.4 ka period the most apparent changes in variability occurred in the range 2.5–4.0 ka. Frequency modulation appears to have occurred regularly over the whole period of record. The pattern of changes, together with amplitude modulation, is much clearer in the Pleistocene section. Less strongly developed, but appearing in both $\delta^{18}O$ and $\delta^{13}C$ records for Makapansgat, is an oscillation in climate at around 0.75–1.25 ka, hereafter called the quasi-1.0 ka oscillation. It underwent considerable frequency modulation with the shortest period of around 750 years occurring earlier than 20 ka and the longest period at around the time of the Early Holocene. At the higher-frequency end of the variability spectrum for the Makapansgat record, a clear ~100-year oscillation is evident. First reported for the last 3.5 ka for the T7 stalagmite (Tyson et al., 2002a), the oscillation is confirmed (though in a weaker form) in the T8 data and is present intermittently throughout the last 24.4 ka.

4. Discussion

4.1. The Makapansgat record

Variation in $\delta^{18}O$ in speleothems is governed by the $\delta^{18}O$ composition of the feeding water, which is, in turn, determined largely by isotope effects in precipitation, including moisture source, air temperatures and storm tracks. It is further governed by the temperature-dependent fractionation factor between the water and

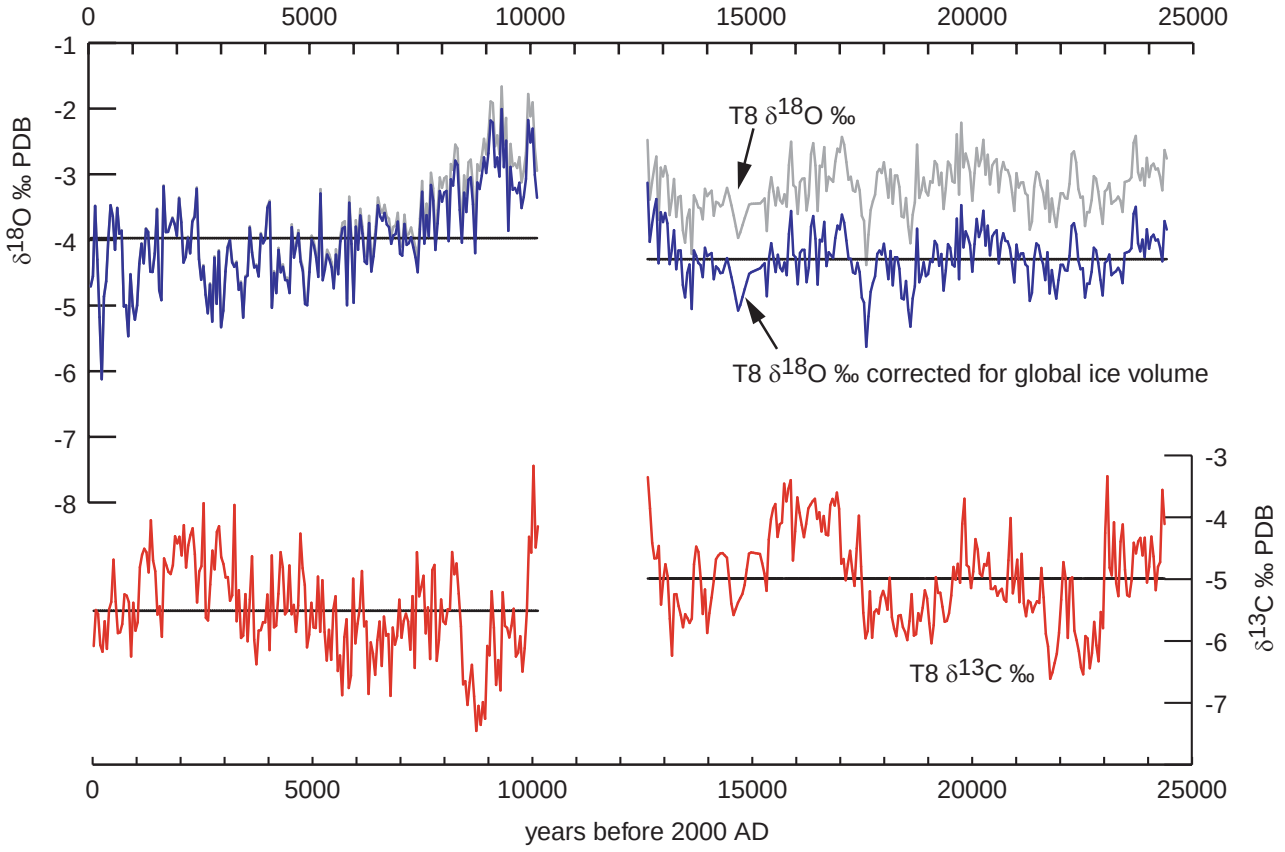

Fig. 5. The Makapansgat T8 $\delta^{18}O$ and $\delta^{13}C$ records for the last 24.4 ka years resolved at 50-year intervals. The aragonite section (0–12.7 ka) has been corrected by −0.6‰ for $\delta^{18}O$ and by −1.8‰ for $\delta^{13}C$ to be comparable with the calcite section (12.7–24.4 ka). In addition, the $\delta^{18}O$ record has been corrected for global ice volume following Guilderson et al. (2001).

the carbonate (Schwarcz, 1986; Lauritzen, 1995). If the $\delta^{18}O$ composition of both the carbonate (c) and its feeding water (w) is known, then temperatures can be estimated using the (Craig, 1965) equation

$$T = 16.9 - 4.2(\delta^{18}O_c - \delta^{18}O_w) + 0.13(\delta^{18}O_c - \delta^{18}O_w)^2. \quad (1)$$

The overarching problem in speleothem isotope studies is the estimation of past dripwater $\delta^{18}O$ composition. In this study, $\delta^{18}O$ ratios from groundwater samples represent average values integrated over several thousands of years. It is unlikely that $\delta^{18}O$ ratios in precipitation have remained stable over such long periods. Consequently, it is not possible to use these average values for estimating temperature variations at the 9–50-year resolution of the Makapansgat $\delta^{18}O$ record. However, it is possible to use the mean values of $\delta^{18}O$ ratios of carbonate and groundwater for the Holocene and Late Pleistocene to obtain an estimate of the temperature difference between the two periods. Given that the Holocene mean values for carbonate (corrected to calcite values) and water are –3.86‰ and –4‰, respectively, and those for the Late Pleistocene are –3.21‰ and –4.8‰, mean temperatures of 16.3°C and 10.6°C can be derived for the Holocene and Late Pleistocene. The difference of 5.7°C compares well with previous estimates of 5–6°C obtained from analyses of dissolved gases from fossil aquifers in South Africa and Namibia (Heaton et al., 1986; Stute and Talma, 1998).

The assumption that the $\delta^{18}O$ composition of rainwater has remained constant at finer timescales in the past may be tested by comparing temperatures calculated from the groundwater and speleothem data, using Eq. (1), with the observed meteorological record for the last century (Fig. 7). The curve thus constructed shows a *cooling* of 5°C from 1950 to the present, in contrast to an observed warming of nearly 1°C for the same period. It may be concluded that $\delta^{18}O$ shifts in rain have overprinted the temperature-dependent fractionation from seepage water to carbonate, implying considerable variation in the $\delta^{18}O$ content of the rain. The oxygen isotope composition of precipitation is controlled by Rayleigh distillation of atmospheric vapour, driven primarily by changes in air-mass temperature (Rozanski et al., 1993). We propose that the observed variability in $\delta^{18}O$ is probably a consequence of changes in the frequency of intense convective high-altitude storm events, on the one hand, and persistent mid-altitude rain during wetter seasons. Convective rain and hail

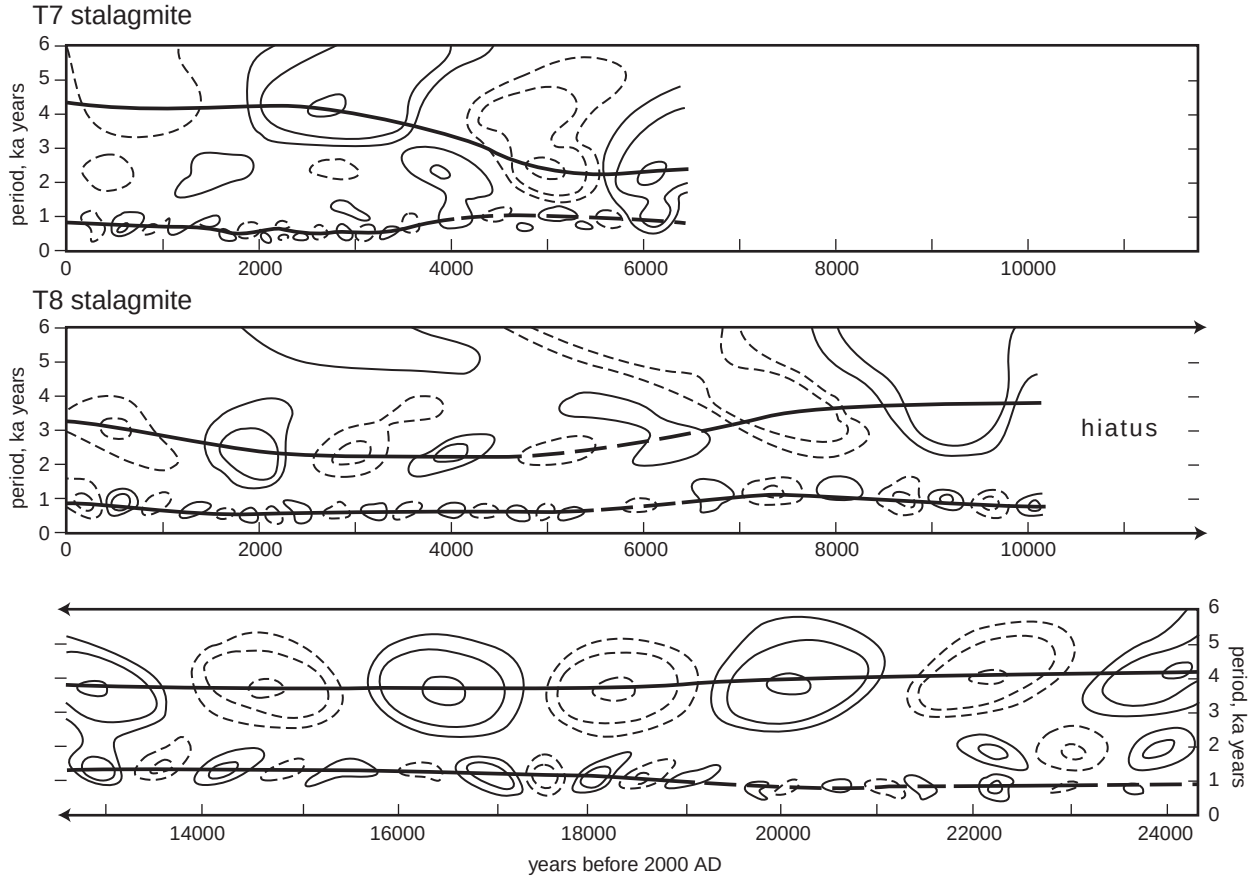

Fig. 6. Wavelet analysis of the 6600-year T7 and 24,400-year T8 $\delta^{18}O$ stalagmite records from the Makapansgat Valley using the Morelet wavelet. Contours are bounded by values of −1.7 to +1.6 in the top panel, by values of −3.1 to +3.7 in the middle panel and by values of −2.5 to +2.4 in the lower panel; positive continuous wavelet transform coefficients are enclosed by solid lines, negative coefficients by broken lines.

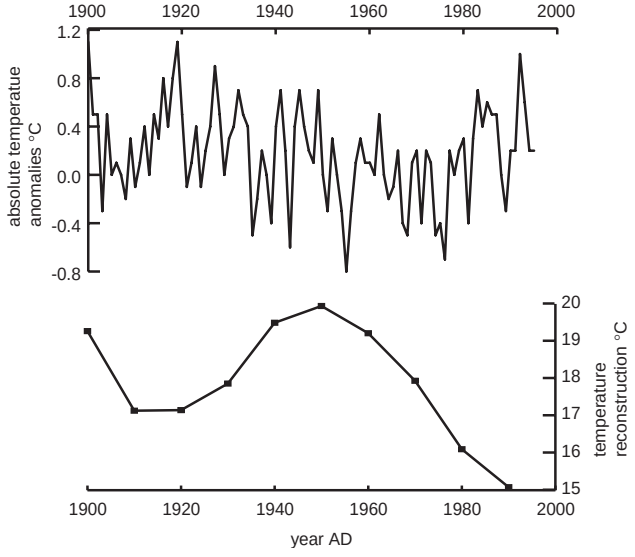

Fig. 7. Twentieth century observed temperature anomalies from the 1960–1990 normal (upper) and the speleothem-derived temperature reconstruction (lower) based on the assumption that precipitation $\delta^{18}O$ has been constant.

originating in the upper troposphere is markedly depleted in $\delta^{18}O$ (Rozanski et al., 1993). The frequency of such storms increases significantly during relatively dry summers (Harrison, 1986) that are associated with the equatorward expansion of the atmospheric circumpolar vortex leading to cooler, drier conditions over the summer rainfall region of South Africa. With the poleward expansion of tropical circulations that accompanies a contraction of the vortex, warmer, wetter conditions prevail (Tyson, 1986; Tyson and Preston-Whyte, 2000). This generalisation does not preclude different combinations of conditions, such as warm and dry, as the dynamics of the atmosphere gave rise to different responses that masked the expanding–contracting vortex effect for extended periods of time. Support for the notion of an expanding–contracting circumpolar vortex is evident from the Antarctic Taylor Dome sodium (salt) record (see later in Fig. 9), which shows a severe weakening of the vortex beginning at around 16 ka and a reversion to the modern-day limit at around 12 ka (Steig et al., 2000).

Changes in the Makapansgat record are therefore ascribed to changes in the $\delta^{18}O$ content of precipitation. For some time it has been known that palaeoclimatic changes in precipitation have resulted from changes in the relative balance of tropically induced rainfall and that originating in the westerly disturbance-associated expansion of the circum-Antarctic atmospheric vortex (Tyson, 1986; Cockroft et al., 1987). In wetter periods, the high frequency of persistent warm rainfall from middle-level stratiform cloud bands is assumed to produce less ^{18}O depletion in the rain than that occurs in dry times. During drier spells, annual average rainfall is less than in wet years, but thunderstorms and hail increase in frequency, as may the rainfall amount in single rainfall events. Thus, both the rainfall type (storms, hail) and the amount effect (more with a single event, but less on an annual basis) may contribute to lower $\delta^{18}O$ values. The most plausible and internally consistent interpretation of the Makapansgat $\delta^{18}O$ record is that higher $\delta^{18}O$ reflects *generally* warmer, wetter conditions while lower values imply cooler, drier conditions. We have considered the alternative interpretation that lower $\delta^{18}O$ values are caused by the amount effect and indicate generally wetter conditions as is suggested by data available from the GNIP data base on the isotopic composition of precipitation in Pretoria (IAEA/WMO, 1998). This explanation is rejected on the basis that, first, it is not consistent with the general atmospheric circulation pattern described above and, secondly, it is not compatible with the observed positive correlation between measured regional temperatures and $\delta^{18}O$ in the T7 stalagmite for the last 100 years (Lee-Thorp et al., 2001), nor with the observed correlation between measured regional temperatures/precipitation and stalagmite colour/layer thickness and $\delta^{18}O$ (Holmgren et al., 1999). These independent lines of evidence provide strong confirmation that lighter $\delta^{18}O$ is representative of generally drier, colder conditions in the Makapansgat Valley.

It is apparent that a drastic and abrupt change in climate/environment occurred at 12.7 ka: a sharp change in crystal form from calcite to aragonite was followed by a 2.5 ka hiatus after which higher growth rates, higher concentrations of uranium and enrichment of stable isotopes are observed in T8. The shift in stalagmite mineralogy indicates the breaching of a threshold. The balance between the two forms is controlled both by Mg content and temperature/evaporation (Murray, 1954). Since Mg is available from the dolomite bedrock, it may be concluded that, in this case, temperature or evaporation forced the mineralogical change. After correction for global ice volume, the mean $\delta^{18}O$ value for 24.4–12.7 ka is 0.3‰ lower than the Holocene mean value (Fig. 5). The unexpectedly small change in $\delta^{18}O$, despite a mean temperature change of 5.7°C between Late Pleistocene and Early Holocene, results from the temperature-dependent fractionation factor between water and calcite dampening the $\delta^{18}O$ signal in precipitation.

Speleothem $\delta^{13}C$ signals reflect the isotopic composition of the soil carbonate, which in turn depends on type of vegetation, but the signal is also influenced by carbon bedrock composition and degassing processes (Schwarz, 1986; Baker et al., 1997). The excellent replication of the T7 and T8 $\delta^{13}C$ records suggests that $\delta^{13}C$ provides a robust indicator of local vegetation conditions. Furthermore, their close correspondence to the Late Holocene trend in $\delta^{13}C$ from the Cango Cave stalagmite in southernmost South Africa (Talma and Vogel, 1992) indicates the presence of a regional signal that transcends local effects. Speleothem carbonate with $\delta^{13}C$ values of about −13‰ reflects an environment dominated by vegetation following the C_3 photosynthetic pathway (including trees, small shrubs, etc.), whereas carbonates with $\delta^{13}C$ values around +1‰ denote a pure grassy C_4-biomass (Talma and Vogel, 1992). C_4 grasses are adapted to high radiation and temperatures in the growing season and grow preferentially where growing season temperatures are above 22°C and minima are not less than 8°C (Vogel et al., 1978; Ehleringer et al., 1997). Furthermore, C_4 grasses out-compete C_3 grasses when atmospheric CO_2 levels are low (Cerling et al., 1997; Ehleringer et al., 1997). Variations in $\delta^{13}C$ thus reflect changes in atmospheric CO_2, temperature, moisture conditions and seasonality of rainfall. The stalagmite $\delta^{13}C$ content, varying between ca –3.2‰ and –6.5‰ (Fig. 5), implies a continuous, significant presence of C_4 grasses. In this context, small amplitude short-term variations are inferred to reflect changes in the relative proportion of C_4 grasses. Higher $\delta^{13}C$ values in the stalagmite indicate good grass cover and therefore optimal summer rainfall conditions, while low values most probably indicate sparse grass cover associated with drier conditions, although this may not be true in every instance. The slightly higher $\delta^{13}C$ average for the Pleistocene part of the record is probably a reflection of lower atmospheric CO_2 levels in which C_4 grasses are favoured. This interpretation is consistent with pollen records at Wonderkrater, which show low Pleistocene woody components, but higher proportion of woody vegetation in the Holocene (Scott, 1982).

4.2. Palaeoclimatic inferences and comparison with other records

The Late Pleistocene Makapansgat stalagmite record indicates drier conditions, lower temperatures and sparser grass cover at about 23–21, 19.5–17.5 and 15–13.5 ka (Fig. 5). Both the Makapansgat $\delta^{18}O$ record and a pollen-derived temperature index from nearby Wonderkrater (Fig. 1) (Scott, 1999), based on a new age model (Scott et al., submitted), show rapid warming

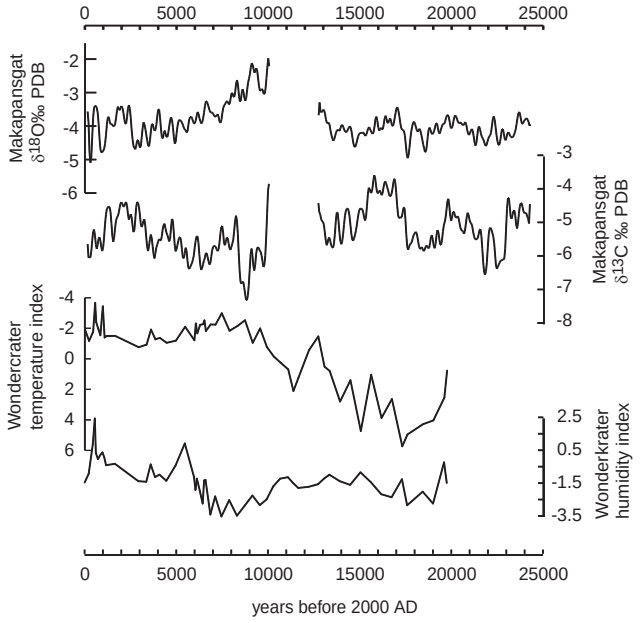

Fig. 8. A regional comparison of the Makapansgat 50-year interval stable isotope records (smoothed with a 9-term binomial filter) with Wonderkrater pollen-derived temperature and humidity indices (Scott, 1999).

after a subdued cold event at 17.5 ka, a return to colder conditions around 15 ka and renewed warming after about 13.5 ka (Fig. 8). Maximum cooling occurred at 17.5 ka with the Wonderkrater pollen sequence indicating a 1000 m drop in vegetation zones, i.e. depression by 5–6°C (Scott, 1982). These findings accord with various less detailed regional proxy records indicating generally drier and colder conditions at this time (Partridge, 1997; Thomas et al., 2000).

Bearing in mind the large age uncertainties for the oldest part of the Makapansgat record, the record can be tentatively compared with others in regions beyond South Africa. The maximum drying and cooling at 17.5 ka precedes the Heinrich 1 event and corresponds with similar conditions reflected in the Taylor Dome $\delta^{18}O$ (Steig et al., 2000) (Fig. 9) and Vostok deuterium (Blünier et al., 1998) ice-core records and by lowstands in tropical Lake Victoria (Stager et al., 2002). The rapid warming and associated wetter conditions beginning after 17.5 ka correspond to similar trends in the Southern Hemisphere polar and tropical ice-core records (Thompson et al., 1995; Blünier et al., 1998; Steig et al., 2000). Concurrent warming is observed in terrestrial lake sediment records from southern African mid- to low-latitudes (Gasse and Van Campo, 1998; Johnson et al., 2002); this hemispheric signal apparently leading that in Northern Hemisphere records by about 2.0 ka years. The return to colder/drier conditions in the stalagmite record, from 15 to 13.5 ka, appears to be a local reflection of the Antarctic Cold Reversal recorded in ice cores from Antarctica (e.g. Blunier et al., 1998) with the exception of the Taylor Dome record (Steig et al., 2000; Fig. 9).

The hiatus from 12.7 to 10.2 ka precludes the reconstruction of environmental conditions based on isotopic variations, but the Wonderkrater temperature index shows an interruption in the warming trend centred on 11.3 ka (Fig. 8). High abundance of the pollen taxa Chenopodiaceae and Amaranthaceae suggests the prevalence of strongly evaporative, but not necessarily low-rainfall, conditions between ca 12 and 10 ka (Scott, 1982; Scott and Holmgren, submitted). The hiatus in Makapansgat stalagmite growth probably reflects the cessation of drip coincident with the onset of these conditions. Drier environments have been inferred in many regions in Africa during this interval, which in northern Europe and elsewhere is defined as the Younger Dryas chronozone. Low lake levels are observed in Lake Victoria at around 12.5 ka (Stager et al., 2002) and in northern Africa at around 12.4 ka (Gasse, 2000). Both cool and dry conditions between 12 and 10.3 ka are suggested by low mass accumulation rate of biogenic silica in Lake Malawi (Johnson et al., 2002); this interval was followed by an abrupt reversion to warmer wetter Holocene conditions and increasing mass accumulation rates. All these findings accord well with the South African record of changes. However, the explanation of the Lake Malawi changes being forced by a southern migration of the ITCZ during Late Pleistocene times (and hence more northerly winds over northern Lake Malawi) flies in the face of the proposed compression of the subtropical high-pressure belts towards the equator with equatorward expansion of the circumpolar vortex during glacial times over southern Africa and elsewhere (Lancaster, 1981, 2000). Other lake records from equatorial and northern Africa indicate, however, that humid conditions were established already at ca 11.5 ka (Gasse, 2000) or do not show any evidence at all of dry conditions at the Lateglacial/Holocene transition (Thevenon et al., 2002).

After the hiatus in the T8 stalagmite, the growth rate increased markedly. The Cango Cave stalagmite from southernmost South Africa (Talma and Vogel, 1992) shows a longer hiatus separating the slow growth rates during the Pleistocene from higher rates during the Holocene; the latter indicate amelioration of environmental conditions on a regional scale and a rapid increase in vegetation cover, with a corresponding rise in soil CO_2 production and enhanced bedrock weathering. Both the $\delta^{18}O$ stalagmite record and the Wonderkrater temperature index indicate generally warm conditions between 10 and 6 ka (Fig. 8). This precedes the southern African Holocene altithermal identified in previous studies (Tyson et al., 2001), but accords with the Early Holocene warming documented in Antarctic ice cores (Masson et al., 2000), in marine cores in South Atlantic (Hodell et al., 2001) and in the recently recovered

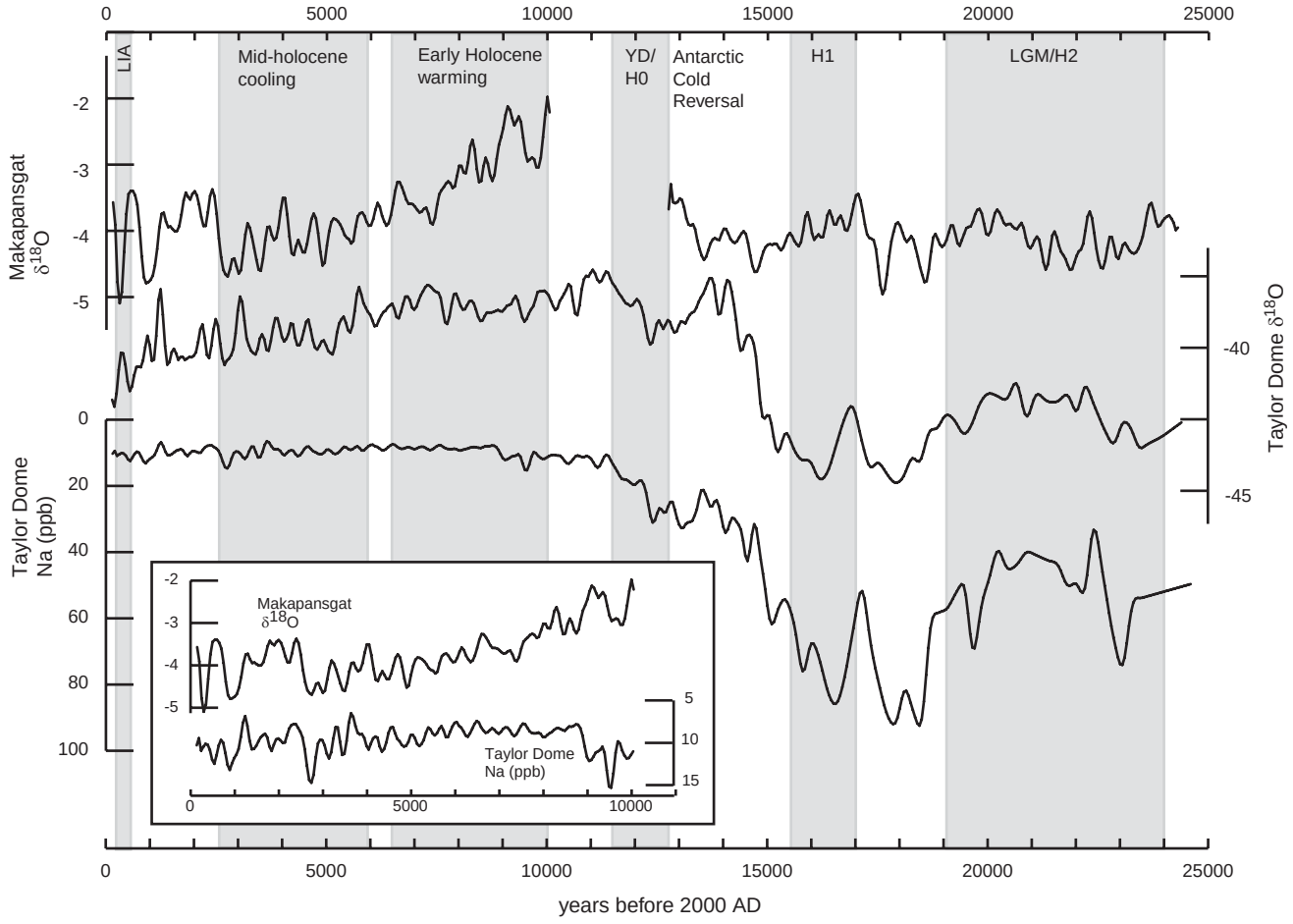

Fig. 9. Comparison of the Makapansgat $\delta^{18}O$ record (50-year intervals and filtered with a 9-term binomial filter) with Taylor Dome $\delta^{18}O$ and sodium records (note inverse scale) (50-year intervals and filtered with a 9-term binomial filter) (Steig et al., 2000). Periods frequently discussed in literature are indicated. Inset figure shows the Taylor Dome sodium record for the Holocene at an enlarged scale, together with the Makapansgat record for easier comparison.

Kilimanjaro ice cores (Thompson et al., 2002). The $\delta^{13}C$ record shows a rapid decrease after 10.2 ka to reach its lowest values at 9–8.4 ka, indicating either increased abundance of C_3 woody vegetation and/or a sharp reduction in C_4 grass cover (Fig. 5). This depletion in $\delta^{13}C$ coincides with an exceptionally white section of the stalagmite, reflecting low organic content and supporting the inference of a vegetation-poor, considerably drier environment. Further evidence for regional desiccation at that time comes from the Wonderkrater pollen record (Fig. 8). After 8.5 ka increased grass cover is indicated at Makapansgat while the Wonderkrater moisture index, which is not dependent on the abundance of grass pollen, suggests a continuation of dry conditions (Fig. 8). Grass pollen does, in fact, increase at Wonderkrater (Scott et al., in preparation), but the pollen spectra indicate a dry, grassy, sparsely wooded ecosystem similar to that of the present semi-arid Kalahari Thornveld. The increase in grass pollen coincides with a sharp decrease in Cyperaceae pollen, indicating shrinking of the Wonderkrater swamp (Scott, 1982; Scott et al., in preparation). Linear dune construction in Zambia at 10–8 ka (O'Connor and Thomas, 1999) argues for more widespread arid conditions. These conditions correspond to a period of low sunspot activity (Stuiver et al., 1998) preceding the "8.2 ka cold event" observed in the North Atlantic (e.g. Alley et al., 1997; deMenocal, 2000; Peterson et al., 2000). They also correspond to a precessional minimum of solar radiation over southern Africa. Equatorial and northern Africa lake records (Gasse, 2000) and the Kilimanjaro ice-core record (Thompson et al., 2002) document a short but strong dry event at about 8.2–8.3 ka within an overall humid Early Holocene.

Both the Makapansgat $\delta^{18}O$ record and the Wonderkrater temperature index show a gradual mid-Holocene cooling between 6 and 3 ka (Figs. 5 and 8). The $\delta^{13}C$ values indicate variable but mostly dry conditions. This part of the T8 $\delta^{18}O$ record does not, however, accord precisely with the corresponding section of stalagmite T7 from the same cave (Fig. 4). Care must therefore be exercised in postulating

teleconnections at that time. However, it should be noted that the T8 record accords with the global evidence for mid-Holocene cooling; in the Southern Hemisphere this temperature decline has been documented in the Antarctic ice cores (Masson et al., 2000), in South Atlantic marine sediments (Hodell et al., 2001) and by glacier expansion in New Zealand (Porter, 2000). The dune record from Zambia (O'Connor and Thomas, 1999) indicates arid conditions at 6–2 ka. Evidence for colder, drier conditions in equatorial Africa comes from the Kilimanjaro ice cores (Thompson et al., 2002) and from glacier expansion on Mt Kenya (Karlén et al., 1999). A biome reconstruction for Africa (Jolly et al., 1998) indicates drier than present conditions in eastern South Africa and equatorial Africa starting at 6 ka (uncalibrated radiocarbon years) at the same time as wetter conditions occurred in northern Africa, suggesting a poleward shift of the north African monsoon. Many lake level records from equatorial and northern Africa, however, suggest that regionally widespread aridity did not occur until after ca 5 ka (Gasse, 2000). The mid-Holocene trend towards lower $\delta^{18}O$ values at Makapansgat mirrors the increase in Na concentrations and lower $\delta^{18}O$ values recorded at Taylor Dome (Steig et al., 2000) (Fig. 9). Once again a strong connection between an enlarged circum-Antarctic vortex and declining temperatures over South Africa is indicated.

The detailed Makapansgat T7 stalagmite record for the last 3 ka has been analysed previously (Tyson et al., 2000) and accords with the lower-resolution Wonderkrater pollen record. High grass and Asteraceae pollen counts support the inference from the isotope record of a cool, grassy environment at 3–2 ka. In contrast, warm, wet conditions and a bushy environment occurred from 1.2 to 0.6 ka. The most recent cool, dry event was that associated with the Little Ice Age from about AD 1500 to 1800.

4.3. Variability

Wavelet analysis of both $\delta^{18}O$ and $\delta^{13}C$ variations in the 24.4 ka Makapansgat record reveals complex changes in climatic variability over the region. In the case of the $\delta^{18}O$ record, the largest changes in variability occurred with quasi-periodicities in the range 2.5–4.0 ka in pre-Holocene times (Fig. 6). Frequency modulation of this oscillation appears to have occurred regularly over the whole period of record. In contrast, amplitude modulation was much more pronounced in pre-Holocene times. Variability with a period of about 4.7 ka has been observed in marine cores from Indian Ocean (Pestiaux et al., 1988) and North Atlantic (Bond et al., 1997; Alley et al., 2001). A global ~2.5 ka oscillation has been reported from glacier fluctuation (Denton and Karlén, 1973), ice cores (Dansgaard et al., 1984; O'Brien et al., 1995) and marine cores (Pestiaux et al., 1988; Rohling et al., 2002). Variability in this range has been ascribed to non-linear responses to the precession cycle (Pestiaux et al., 1988) and solar forcing (Davis et al., 1992; Stuiver et al., 1995), as well as to stochastic resonance of Dansgaard/Oeschger events every 1500 years, or multiples thereof (Ganopolski and Rahmstorf, 2002).

Less strongly developed, but appearing in both $\delta^{18}O$ and $\delta^{13}C$ records for Makapansgat is the oscillation in climate at around 0.75–1.25 ka, the quasi-1-ka oscillation. It underwent considerable frequency modulation with the shortest period of around 750 years occurring earlier than 20 ka and the longest in the Early Holocene. The most pronounced change in the pattern of variability occurred at around 6 ka. At widely separated localities elsewhere in the world, variability with a quasi-period of around 1.0–1.5 ka has been reported by many workers. Monsoonal climates show high-frequency variability with intervals of 1.8, 1.45 and 1.15 ka (Sirocko et al., 1996). North Atlantic deep ocean cores reveal Holocene climatic shifts with a period of 1.5 ± 0.5 ka (Bond et al., 1997, 1999, 2001; Bianchi and McCave, 1999). A faunal record of sea-surface temperature variations off West Africa also suggests variability within the range 1.0–2.0 ka (deMenocal et al., 2000) and geochemical and clay parameters in mineral marine cores from the continental slope off Chile show bands of variability at ~0.9 and 1.5 ka years (Lamy et al., 2001). Eleven ice cores from a variety of coastal and central Antarctic sites typically show oscillations of 0.8–1.2 ka, with a reduced spacing between warm events (~800 years) and an enhanced spacing (~1200 years) during cooler periods (Masson et al., 2000). The Makapansgat record suggests the opposite, in that the highest frequencies (with a quasi-period of ~750 years) occurred earlier than 20 ka and the lowest (~1250 years) during the Early Holocene. Climate oscillations in the range 1.5 ± 0.5 ka have been thought to result from changes in the thermohaline circulation of the North Atlantic and its connectivity with the global thermohaline conveyor (Bond et al., 1997; Bianchi and McCave, 1999), from vegetation-albedo positive feedbacks (deMenocal et al., 2000), from stochastic resonance (Ganopolski and Rahmstorf, 2002) and perhaps most persuasively, from variations of solar output (Stuiver et al., 1995; Bond et al., 2001).

At the higher-frequency end of the spectrum, the ~100-year oscillation, prominent during the first 3500 years of the T7 record (Tyson et al., 2002a), can be discerned weakly and intermittently throughout the 24.4 ka T8 record. It is also observed in long tree-ring records from South Africa and in a run-off record for the Zambezi River at the Victoria Falls (Tyson et al., 2002a). The ~100-year oscillation (often referred to as the ~80-year oscillation) is evident in a number of long records, such as the Greenland Camp Century oxygen

isotope record (Dansgaard et al., 1973), the Nile River flood series (Hameed (1984) quoted in Hoyt and Schatten, 1997), in cosmogenic isotopes in tree-ring series (Hoyt and Schatten, 1997), as well as in central England temperatures (Burroughs, 1992) and Chinese rainfall (Zhu and Wang, 2002). Furthermore, significant variability has been found to reside in the 60–80-year band in simultaneous historical Northern Hemisphere surface air temperature and sea-level pressure (Mann and Park, 1994, 1996), in global sea-surface temperature data (Folland et al., 1998) and in joint empirical orthogonal function analysis of historical sea-surface temperatures and mean sea-level pressures around the globe (Allan, 2000). It has been suggested that the variability at around 100 years may be related to changes in solar output associated with the Gleissberg cycle of around 80 years, which is, in turn, linked to high and low phases of the 11-year solar cycle (Lean et al., 1992, 1996; Hoyt and Schatten, 1993, 1997; Harrison and Shine, 1999). The T8 Makapansgat data indicate that the 100-year rhythm in southern African climates was considerably more long lived than was previously thought to be the case.

4.4. Major forcing mechanisms

Long palaeoenvironmental records within and around southern Africa clearly demonstrate the interplay between Milankovitch solar forcing and influences originating from local components of the global thermohaline system, as well as from elements of the circum-Antarctic atmospheric circulation (Partridge, 2002). Both of the latter forcings probably arise from non-linear responses to orbital influences (Curry and Oppo, 1997), but are separated for the purposes of this discussion. It has been shown that precessional forcing has produced clear climatic responses in the continental interior of southern Africa during the last 200,000 years (Partridge et al., 1997). As the precessional signal weakened, so regional influences became more important, and after about 50 ka climatic changes appear to have been driven increasingly by stadial/interstadial cycles (Partridge, 2002). The precessional low, which occurred at the beginning of the Holocene, is reflected particularly clearly in the antiphase response of African lakes on either side of a line some 10–15° south of the equator: south of this, low lake levels reflect dry conditions associated with the Early Holocene decline in incoming solar radiation, while around the equator and in areas to the north lake levels were high in conformity with a northward shift in the position of the ITCZ (Partridge and Scott, 2000; Tyson and Partridge, 2000). The southern African precessional low is, as must be expected from the more evaporative conditions which it brought, reflected in the Makapansgat Holocene record before about 7 ka. This response of the isotope record to orbital precession is in accord with the findings of Wang et al. (2001) from the longer speleothem time series in China where, however, an inverse correlation is evident because of the Northern Hemisphere location of the site.

The onset of cold stadials at high latitudes is manifested in two ways over southern Africa. The extension of Antarctic sea-ice shifts the oceanic Antarctic Convergence northward; this increases the diameter of the atmospheric circumpolar vortex. At the same time a steepened thermal gradient across Antarctica increases the intensity of the circulation. The net result is an extension northwards of the mid-latitude westerlies and an associated equatorward displacement of the subtropical highs with their attendant weather-suppressing subsidence. At the same time the influence of precessional forcing via the tropical easterlies is diminished. Precipitation responses in the summer rainfall region are a decrease in annual rainfall receipts and an increase in the small winter rainfall component (but without a change in overall seasonality). This atmospheric response is virtually instantaneous.

In the context of the thermohaline circulation, slowing or cessation of the North Atlantic Deep Water formation (e.g., during the Younger Dryas or the first Heinrich event) restricts heat transfer from the western Indian Ocean into the eastern South Atlantic via the Agulhas current (Zonneveld et al., 1997; Lutjeharms et al., 2001). This involves a significant time lag; its effect is to lower sea-surface temperatures along the west coast of southern Africa as well as to amplify and prolong arid interludes, particularly over the western parts of the subcontinent. These oceanic changes are analogous to the millennial-scale, ENSO-like shift in sea-surface temperature distributions that have characterised the tropical Pacific Ocean during the past 3.0–7.0 ka (Koutavas et al., 2002; Stott et al., 2002).

In southern Africa, centennial-scale teleconnections of an ENSO-like character (similar to those observed with individual ENSO occurrences during the period of instrumental record) have been observed between Kenya and South Africa (Tyson et al., 2002b) adding credence to the notion that long-period changes in seawater temperature and salinity variability in the tropical Pacific Ocean may have regional implications and manifestations far beyond the source area.

In the case of the Makapansgat record, these oceanic influences are clearly evident in the intervals of depleted $\delta^{18}O$ which occurred after about 23.5, 19 ka, and again after about 15.5 ka. Similar shifts are observed in the Mozambique Channel marine core record (Bard et al., 1997). In Antarctica, similar trends are observed in the Taylor Dome ice-core record, but at higher amplitudes and not with complete synchronicity (Steig et al., 2000). Shifts in the Makapansgat record appear to lead those in the Antarctic cores. However, the association must be

treated with caution because of the large error limits applicable to the Pleistocene segment of the Makapansgat record.

5. Conclusions

The 24.4 ka, high-resolution and near-continuous Makapansgat T8 record documents climate change in southern Africa from the Lateglacial period through the Holocene. The record has an extremely good chronology for the Holocene and a somewhat less secure, but nonetheless good, dating control for the Pleistocene. Together with the nearby pollen record and groundwater isotope data, the Makapansgat speleothem record provides the basis for a robust high-resolution palaeoclimatic reconstruction for the region.

Mean temperature conditions for the Holocene and Pleistocene have been calculated, using mean oxygen isotope data from the aquifer and the stalagmite. The mean temperature difference is 5.7°C and compares well with similar estimates of 5–6°C in other parts of South Africa and Namibia.

Low Makapansgat $\delta^{18}O$ values place the coolest period of the record at around 17–18 ka preceding the Heinrich 1 event. The Antarctic Cold Reversal is evident and is centred about 13.5 ka. Formerly thought to be unique to southern polar records, this reversal is an event traceable from pole to equator in the Southern Hemisphere. The initiation of strong postglacial warming is clearly evident in the Makapansgat record, but its character is lost in the 2.5 ka hiatus in speleothem growth at 10.2–12.7 ka. This hiatus is coeval with the Younger Dryas or Heinrich 0 event. The neighbouring Wonderkrater pollen record suggests that evaporative conditions prevailed at this time. The Early Holocene is characterised by regionally pervasive dry, evaporative conditions. The more recent Holocene shows an overall trend towards lower $\delta^{18}O$, with a number of sharp negative excursions from about 5.2 ka. Clear mid-Holocene cooling is evident in the Makapansgat T8 record between about 2.5 and 6 ka. Warmer periods occurred between 1 and 2 ka and were followed by a resumption of the declining trend. Evidence for medieval warming is present. The Little Ice Age covered the four centuries between AD 1500 and 1800 and at its maximum at AD 1700 represents the most pronounced negative $\delta^{18}O$ deviation in the entire record.

Superimposed on long-period changes, a spectrum of climatic variability is apparent in the Makapansgat record. Evidence of change at Milankovitch scales is forthcoming. More pronounced is variability in the range 2.5–4.0 ka. During the Pleistocene part of the record amplitude modulation is particularly apparent. Wavelet analysis clearly reveals the continuity of the oscillation despite frequency changes, and illustrates the difficulty of determining the quasi-periodicity of such variability using traditional methods of spectral analysis. Also present in the record is a weaker signal at around 1.0 ka that may be an echo of the Bond cycles reported for the North Atlantic region.

Comparison of the Makapansgat record with the Taylor Dome sodium record corroborates the hypothesis that an expanding–contracting atmospheric circumpolar vortex, by shifting the westerlies and their attendant weather-producing disturbances equatorward and poleward, did much to control the changing patterns of climate over southern Africa over long periods of time. With retreat of tropical circulations equatorward with an expanding vortex, the summer rainfall region of South Africa became cooler and drier (in contrast to the south-western winter rainfall region of the subcontinent which became wetter and cooler). With contraction of the vortex and poleward advance of tropical circulations the opposite occurred.

A clear understanding of earth system functioning from the last glacial onwards is hampered by a paucity of good, high-resolution terrestrial records from the Southern Hemisphere. Such a record is now available from the Makapansgat stalagmites. It allows a detailed interpretation to be made of climatic change and variability in the summer rainfall region of South Africa. The record is robust and representative of a much larger region of southern Africa. Furthermore, the new findings from South Africa provide a vital link in the chain of events that have taken place over the last 24.4 ka years between the tropics of the Southern Hemisphere and high latitudes of Antarctica.

Acknowledgements

The National Research Foundation and Water Research Commission of South Africa and the Swedish Research Council are acknowledged for the financial support given to this research. We wish to acknowledge the contribution of A. Eisenhauer at GEOMAR, Forschungszentrum für marine Geowissenschaften in Kiel for the TIMS-dating. Ice-core data series were obtained from the NOAA World Data Center A Paleoclimatology. Wendy Job composed Figs. 1 and 6.

References

Acocks, J.P.H., 1953. Veld types of South Africa. Memoirs of the Botanical Survey of South Africa 28, 1–192.

Allan, R.J., 2000. ENSO and climate variability in the last 150 years. In: Diaz, H., Markgraf, V. (Eds.), El Niño and the Southern Oscillation: Multiscale Variability, Global and Regional Impacts. Cambridge University Press, Cambridge, pp. 3–56.

Alley, R.B., Mayewski, P.A., Sowers, T., Stuiver, M., Taylor, K.C., Clark, P.U., 1997. Holocene climatic instability: a prominent, widespread event 8200 yr ago. Geology 25 (6), 483–486.

Alley, R.B., Anandakrishnan, S., Jung, P., 2001. Stochastic resonance in the North Atlantic. Paleooceanography 16 (2), 190–198.

Baker, A., Ito, E., Smart, P.L., McEvan, R.F., 1997. Elevated and variable values of ^{13}C in speleothems in a British cave system. Chemical Geology 136, 263–270.

Bard, E., Rostek, F., Sonzogni, C., 1997. Interhemispheric synchrony of the last deglaciation inferred from palaeothermometry. Nature 385, 707–710.

Bianchi, G.G., McCave, I.N., 1999. Holocene periodicity in Norht Atlantice climate and deep-ocean flow south of Iceland. Nature 397, 515–517.

Blunier, T., Chappellaz, J., Schwander, J., Dällenbach, A., Stauffer, B., Stocker, T.F., Raynaud, D., Jouzel, J., Clausen, H.B., Hammer, C.U., Johnsen, S.J., 1998. Asynchrony of Antarctic and Greenland climate change during the last glacial period. Nature 394, 739–743.

Bond, G., Showers, W., Cheseby, M., Lotti-Bond, R., Almasi, P., deMenocal, P., Priore, P., Cullen, H., Hajdas, I., Bonani, G., 1997. A pervasive millennial-scale cycle in North Atlantic Holocene and glacial climates. Science 278, 1257–1266.

Bond, G., Showers, W., Elliot, M., Evans, M., Lotti-Bond, R., Hajdas, I., Bonani, G., Johnson, S., 1999. The North Atlantic's 1–2 kyr climate rhytm: relation to Heinrich events, Dansgard/Oeschger cycles and the Little Ice Age. In: Clark, P.U., Webb, R.S., Keigwin, L.D. (Eds.), Mechanisms of Global Climate Change at Millennial Time Scales, Geophysical Monograph 112, pp. 35–58. American Geophysical Union.

Bond, G., Kromer, B., Beer, J., Muscheler, R., Evans, M.N., Showers, W., Hoffmann, S., Lotti-Bond, R., Hajdas, I., Bonani, G., 2001. Persistent solar influence on north Atlantic climate during the Holocene. Science 294, 2130–2136.

Burroughs, W.J., 1992. Weather Cycles, Real or Imaginary? Cambridge University Press, Cambridge, 201pp.

Cerling, T.E., Harris, J.M., MacFadden, B.J., Leakey, M.G., Quade, J., Eisenmann, V., Ehleringer, J.R., 1997. Global vegetation change through the Miocene/Pliocene boundary. Nature 389, 153–158.

Cheng, H., Edwards, R.L., Hoff, J., Gallup, C.D., Richards, D.A., Asmerom, Y., 2000. The half-lives of uranium-234 and thorium-230. Chemical Geology 169, 17–33.

Cockroft, M.J., Wilkinson, M.J., Tyson, P.D., 1987. The application of a present-day climatic model to the Late Quaternary in southern Africa. Climatic Change 10, 161–191.

Cohen, J., 1990. Things I have learned (so far). American Psychology 45, 378–399.

Craig, H., 1965. The measurements of oxygen isotope palaeotemperature: stable isotopes in oceanographic studies and paleotemperatures. In: Tongiori, E. (Ed.), Proceedings of the Third Spoleto Conference, Spoleto, Italy. Sischi and Figli, Pisa, pp. 161–182.

Curry, W.B., Oppo, D.W., 1997. Synchronous, high-frequency oscillations in tropical sea surface temperatures and North Atlantic Deep Water production during the last glacial cycle. Paleoceanography 12 (1), 1–14.

Dansgaard, W., Johnsen, S.J., Clausen, H.B., Langway, C.C., 1973. Climate record revealed by the Camp Century ice core. In: Turekian, K.K. (Ed.), The Late Cenozoic Ice Ages. Yale University Press, New Haven, pp. 43–44.

Dansgaard, W., Johnsen, S.J., Clausen, H.B., Dahl-Jensen, D., Gundestrup, N., Hammer, C.U., 1984. North Atlantic climatic oscillations revealed by deep Greenland ice cores. In: Ewing, M. (Ed.), Climate Processes and Climate Sensitivity, Geophysical Monograph 29, Vol. 5, pp. 288–298. American Geophysical Union.

Davis, O.K., Jirikowic, J., Kalin, R.M., 1992. Radiocarbon record of solar variability and Holocene climatic change in coastal southern California. In: Redmond, K.T. (Ed.), Proceedings of the Eighth Annual Pacific Climate (PACLIM) Workshop, March 10–13 1991, California Department of Water resources, Interagency Ecological Studies Program Technical Report 31, pp. 19–33.

deMenocal, P., Ortiz, J., Guilderson, T., Sarnthein, M., 2000. Coherent high- and low-latitude climate variability during the Holocene warm period. Science 288, 2198–2202.

Denton, G., Karlén, W., 1973. Holocene climatic variations—their pattern and possible cause. Quaternary Research 3, 155–205.

Ehleringer, J.R., Cerling, T.E., Helliker, B.R., 1997. C_4 photosynthesis, atmospheric CO_2, and climate. Oecologia 112, 285–299.

Flueck, J.A., Brown, T.J., 1993. Criteria and methods for performing and evaluating solar-weather studies. Journal of Climate 6, 373–385.

Folland, C.K., Parker, D.E., Colman, A.W., Washington, R., 1998. Large scale modes of ocean surface temperature since the late nineteenth century. Climate Research Technical Note CRTN18, Hadley Centre, Meteorological Office, Bracknell, UK, 21pp.

Ganopolski, A., Rahmstorf, S., 2002. Abrupt glacial climate changes due to stochastic resonance. Physical Review Letters 88 (3), 038501.

Gasse, F., 2000. Hydrological changes in the African tropics since the Last Glacial Maximum. Quaternary Science Reviews 19, 189–211.

Gasse, F., Van Campo, E., 1998. A 40,000-yr pollen and diatom record from Lake Tritrivakely, Madagascar, in the southern tropics. Quaternary Research 49, 299–311.

Grossman, E.L., Ku, T.-L., 1986. Oxygen and carbon isotope fractionation in biogenic aragonite: temperature effects. Chemical Geology 59, 59–74.

Guilderson, T.P., Fairbanks, R.G., Rubenstone, J.L., 2001. Tropical Atlantic coral oxygen isotopes: glacial–interglacial sea surface temperatures and climate change. Marine Geology 172, 75–89.

Harrison, M.S.J., 1986. A synoptic climatology of South African rainfall variability. Unpublished Ph.D. Thesis, University of the Witwatersrand, Johannesburg, 341pp.

Harrison, R.G., Shine, K.P., 1999. A review of recent studies of the influence of solar changes on the earth's climate. Technical Note 6, Hadley Centre, UK Meteorological Office, Bracknell, 64pp.

Heaton, T.H.E., Talma, A.S., Vogel, J.C., 1986. Dissolved gas paleotemperatures and ^{18}O variations derived from groundwater near Uitenhage, South Africa. Quaternary Research 25, 79–88.

Hodell, D.A., Kanfoush, S.L., Shemesh, A., Crosta, X., Charles, C.D., Guilderson, T.P., 2001. Abrupt cooling of Antarctic surface waters and sea ice expansion in the South Atlantic sector of the Southern Ocean at 5000 cal yr B.P. Quaternary Research 56, 191–198.

Holmgren, K., Karlén, W., Lauritzen, S.E., Lee-Thorp, J.A., Partridge, T.C., Piketh, S., Repinski, P., Stevenson, C., Svanered, O., Tyson, P.D., 1999. A 3000-year high-resolution record of palaeoclimate for north-eastern South Africa. The Holocene 9 (3), 295–309.

Hoyt, D.V., Schatten, K.H., 1993. A discussion of plausible solar irradiance variations, 1700–1992. Journal of Geophysical Research 98, 18895–18906.

Hoyt, D.V., Schatten, K.H., 1997. The Role of the Sun in Climate Change. Oxford University Press, New York, 279pp.

IAEA, 1992. Statistical Treatment of Data on Environmental Isotopes in Precipitation. Technical Reports Series. International Atomic Energy Agency, Vienna, p. 331.

IAEA/WMO, 1998. Global network for isotopes in precipitation. The GNIP database. Release 3 October 1999: URL: http://www.iaea.org/programs/ri/gnip/gnipmain.htm (11/2000).

Jaffey, A.H., Flynn, K.F., Glendenin, L.E., Bently, W.C., Essling, A.M., 1971. Precision measurements of half-lives and specific activities of ^{235}U and ^{238}U. Physical Review Letters C 4, 1889–1906.

Johnson, T.C., Brown, E.T., McManus, J., Barry, S., Barker, P., Gasse, F., 2002. A high-resolution paleoclimate record spanning the past 25,000 years in southern east Africa. Science 296, 113–132.

Jolly, D., et al., 1998. Biome reconstruction from pollen and plant macrofossil data for Africa and the Arabian Penninsula at 0 and 6000 years. Journal of Biogeography 25, 1007–1027.

Karlén, W., Fastook, J.L., Holmgren, K., Malmström, M., Matthews, J.A., Odada, E., Risberg, J., Rosqvist, G., Sandgren, P., Shemesh, A., Westerberg, L.-O., 1999. Glacier fluctuations on Mount Kenya since 6000 Cal. years BP: implications for Holocene climatic change in Africa. Ambio 28, 409–418.

Koutavas, A., Lynch-Stieglitz, J., Marchitto, T.M., Sachs, J.P., 2002. El Niño-like patterns in ice age tropical Pacific sea surface temperature. Science 297, 226–230.

Lamy, F., Hebbeln, D., Röhl, U., Wefer, G., 2001. Holocene rainfall variability in southern Chile: a marine record of latitudinal shifts of the Southern Westerlies. Earth and Planetary Science Letters 185, 369–382.

Lancaster, N., 1981. Palaeoenvironmental implications of fixed dune systems in southern Africa. Palaeogeography, Palaeoclimatology, Palaeoecology 33, 327–346.

Lancaster, N., 2000. Eolian deposits. In: Partridge, T.C., Maud, R.R. (Eds.), The Cenozoic of Southern Africa. Oxford University Press, New York, pp. 73–87.

Lau, K.-M., Weng, H.-Y., 1995. Climate signal detection using wavelet transform: how to make a time series sing. Bulletin of the American Meteorological Society 76, 2391–2402.

Lauritzen, S.E., 1995. A high-resolution palaeotemperature proxy record during the last interglaciation in Norway from speleothems. Quaternary Research 43, 133–146.

Lean, J., 1996. Reconstructions of past solar variability. In: Jones, P.D., Bradley, R.S., Jouzel, J. (Eds.), Climatic Variations and Forcing Mechanisms of the Last 2000 Years. NATO ASI Series 1, Vol. 41. Springer, Berlin, pp. 519–532.

Lean, J., Skumanich, A., White, O., 1992. Estimating the sun's radiative output during the Maunder minimum. Geophysical Research Letters 19, 1591–1594.

Lee-Thorp, J.A., Holmgren, K., Lauritzen, S.E., Linge, H., Moberg, A., Partridge, T.C., Stevenson, C., Tyson, P., 2001. Rapid climate shifts in the southern African interior throughout the mid to Late Holocene. Geophysical Research Letters 28, 4507–4510.

Lutjeharms, J.R.E., Monteiro, P.M.S., Tyson, P.D., Obura, D., 2001. The oceans around southern Africa and regional effects of global change. South African Journal of Science 97, 119–130.

Mann, M.E., Park, J., 1994. Global-scale modes of surface temperature variability on interannual to century time scales. Journal of Geophysical Research 99, 25819–25833.

Mann, M.E., Park, J., 1996. Joint spatiotemporal modes of surface temperature and sea level pressure variability in the Northern Hemisphere during the last century. Journal of Climate 9, 2137–2162.

Masson, V., Vimeux, F., Jouzel, J., Morgan, V., Delmotte, M., Ciais, P., Hammer, C., Johnsen, S., Lipenkov, V.Y., Mosley-Thompson, E., Petit, J.R., Steig, E.J., Stievenard, M., Vaikmae, R., 2000. Holocene climate variability in Antarctica based on 11 ice-core isotopic records. Quaternary Research 54, 348–358.

Murray, J.W., 1954. Deposition of calcite and aragonite in caves. Journal of Geology 62, 481–492.

Nicholls, N., 2000. The insignificance of significance testing. Bulletin of the American Meteorological Society 81, 981–986.

O'Brien, S.R., Mayewski, P.A., Meeker, L.D., Meese, D.A., Twickler, M.S., Whitlow, S.I., 1995. Complexity of Holocene climate as reconstructed from a Greenland ice core. Science 270, 1962–1964.

O'Connor, P.W., Thomas, D.S.G., 1999. The timing and environmental significance of Late Quaternary linear dune development in western Zambia. Quaternary Research 52, 44–55.

Partridge, T.C., 1997. Cainozoic environmental change in southern Africa, with special emphasis on the last 200,000 years. Progress in Physical Geography 21 (1), 3–22.

Partridge, T.C., 2002. Were Heinrich events forced from the Southern Hemisphere? South African Journal of Science 98, 43–46.

Partridge, T.C., Scott, L., 2000. Lakes and pans. In: Partridge, T.C., Maud, R.R. (Eds.), The Cenozoic of Southern Africa. Oxford University Press, New York, pp. 145–161.

Partridge, T.C., deMenocal, P.B., Lorentz, S.A., Paiker, M.J., Vogel, J.C., 1997. Orbital forcing of climate over South Africa: a 200,000-year rainfall record from the Pretoria Saltpan. Quaternary Science Reviews 16, 1125–1133.

Pestiaux, P., Van Der Mersch, I., Berger, A., Duplessy, J.C., 1988. Paleoclimatic variability at frequencies ranging from 1 cycle per 10,000 years to 1 cycle per 1000 years: evidence for a nonlinear behaviour of the climate system. Climate Change 12, 9–37.

Peterson, L.C., Haug, G.H., Hughen, K.A., Röhl, U., 2000. Rapid changes in the hydrologic cycle of the tropical Atlantic during the last glacial. Science 290, 1947–1951.

Porter, S.C., 2000. Onset of neoglaciation in the Southern Hemisphere. Journal of Quaternary Science 15, 395–408.

Rohling, E.J., Mayewski, P.A., Abu-Zied, R.H., Casford, J.S.L., Hayes, A., 2002. Holocene atmosphere–ocean interactions: records from Greenland and the Aegean Sea. Climate Dynamics 18, 587–593.

Rozanski, K., Araguás-Araguás, L., Gonfiantini, R., 1993. Isotopic patterns in modern global precipitation. In: Swart, P.P., Lohmann, K.C., McKenzie, J., Savin, S. (Eds.), Climate change in Continental Isotopic Records. Geophysical Monograph 78, pp. 1–36. American Geophysical Union.

Scholes, R.J., 1997. Savanna. In: Cowling, R.M., Richardson, D.M., Pierce, S.M. (Eds.), Vegetation of Southern Africa. Cambridge University Press, Cambridge, pp. 258–277.

Schulze, B.R., 1984. Climate of South Africa, Part 8: General Survey, 5th Edition, WB 28. South African Weather Bureau, Pretoria, 330pp.

Schwarcz, H.P., 1986. Geochronology and isotopic geochemistry of speleothems. In: Fritz, P., Fontes, J.Ch. (Eds.), Handbook of Environmental Isotope Geochemistry, Vol. 2. Elsevier, Amsterdam, pp. 271–303.

Scott, L., 1982. A Late Quaternary pollen record from the Transvaal bushveld, South Africa. Quaternary Research 17, 339–370.

Scott, L., 1999. The vegetation history and climate in the Savanna Biome, South Africa since 190,000 ka: a comparison of pollen data from the Tswaing Crater (the Pretoria Saltpan) and Wonderkrater. Quaternary International 57, 215–223.

Sirocko, F., Garbe-Schönberg, D., McIntyre, A., Molfino, B., 1996. Teleconnections between the subtropical monsoons and high-latitude climates during the last deglaciation. Science 272, 526–529.

Stager, J.C., Mayewski, P.A., Meeker, L.D., 2002. Cooling cycles, Heinrich event 1 and the desiccation of Lake Victoria. Palaeogeography, Palaeoclimatology, Palaeoecology 183, 169–178.

Steig, E.J., Morse, D.L., Waddington, E.D., Stuiver, M., Grootes, P.M., Mayewski, P.A., Twickler, M.S., Whitlow, S.I., 2000. Wisconsian and Holocene climate history from an ice core at Taylor Dome, Western Ross Embament, Antarctica. Geografiska Annaler 82A (2–3), 213–235.

Stott, L., Poulsen, C., Lund, S., Thunell, R., 2002. Super ENSO and global climate oscillations at millennial time scales. Science 297, 222–226.

Stuiver, M., Grootes, P.M., Braziunas, T.F., 1995. The GISP2 $\delta^{18}O$ climate record of the past 16,500 years and the role of the sun, ocean, and volcanoes. Quaternary Research 44, 341–354.

Stuiver, M., Reimer, P.J., Bard, E., Beck, J.W., Burr, G.S., Hughen, K., Kromer, B., McCormac, G., van der Plicht, J., Spurk, M., 1998. INTCAL98 radiocarbon age calibration, 24,000–0 cal BP. Radiocarbon 40 (3), 1041–1083.

Stute, M., Talma, A.S., 1998. Glacial temperatures and moisture transport regimes reconstructed from noble gases and $\delta^{18}O$,

Stampriet aquifer, Namibia. In: Isotope Techniques in the Study of Environmental Change: Proceedings of a Symposium in Vienna, 14–18 April 1997. IAEA, Vienna, pp. 307–318.

Talma, A.S., Vogel, J.C., 1992. Late Quaternary paleotemperatures derived from a speleothem from Cango Caves, Cape Province, South Africa. Quaternary Research 37, 203–213.

Tarutani, T., Clayton, R.N., Mayeda, T.K., 1969. The effect of polymorphism and magnesium substitution on oxygen isotope fractionation between calcium carbonate and waer. Geochimica et Cosmochimica 33, 987–996.

Thevenon, F., Williamson, D., Taieb, M., 2002. A 22 kyr BP sedimentological record of Lake Rukwa (8°S, SW Tanzania): environmental, chronostratigraphic and climatic implications. Palaeogeography, Palaeoclimatology, Palaeoecology 187, 285–294.

Thomas, D.S.G., O'Connor, P.W., Bateman, M.D., Shaw, P.A., Stokes, S., Nash, D.J., 2000. Dune activity as a record of Late Quaternary aridity in the Northern Kalahari: new evidence from northern Namibia interpreted in the context of regional arid and humid chronologies. Palaeogeography, Palaeoclimatology, Palaeoecology 156, 243–259.

Thompson, L.G., Mosley-Thompson, E., Davis, M.E., Lin, P.-N., Henderson, K.A., Cole-Dai, J., Bolzan, J.F., Liu, K.-b., 1995. Late glacial stage and Holocene tropical ice core records from Huascaran, Peru. Science 269, 46–50.

Thompson, L.G., Mosley-Thompson, E., Davis, M.E., Lin, P.-N., Henderson, K.A., Brecher, H.H., Zagorodnov, V.S., Mashiotta, T.A., Lin, P.-N., Mikhalenko, V.N., Hardy, D.R., Beer, J., 2002. Kilimanjaro ice core records: evidence of Holocene climate change in tropical Africa. Science 298, 589–593.

Torrence, C., Compo, G.P., 1998. A practical guide to wavelet analysis. Bulletin of the American Meteorological Society 79, 61–78.

Tyson, P.D., 1986. Climatic Change and Variability in Southern Africa. Oxford University Press, Oxford, 220pp.

Tyson, P.D., Partridge, T.C., 2000. Evolution of Cenozoic climates. In: Partridge, T.C., Maud, R.R. (Eds.), The Cenozoic of Southern Africa. Oxford University Press, New York, pp. 371–387.

Tyson, P.D., Preston-Whyte, R.A., 2000. The Weather and Climate of Southern Africa. Oxford University Press, Cape Town, 396pp.

Tyson, P.D., Karlén, W., Holmgren, K., Heiss, G.A., 2000. The little ice age and medieval warming in South Africa. South African Journal of Science 96, 121–126.

Tyson, P.D, Odada, E.O., Partridge, T.C., 2001. Late Quaternary environmental change in southern Africa. South African Journal of Science 97, 139–150.

Tyson, P.D., Cooper, G.R., McCarthy, T.S., 2002a. Millennial to multi-decadal variability in the climate of southern Africa. International Journal of Climatology 22, 1105–1117.

Tyson, P.D., Lee-Thorp, J., Holmgren, K., Thackeray, J.F., 2002b. Changing gradients of climate change in southern Africa during the past millennium: their implications for population movements. Climatic Change 52, 129–135.

Verhagen, B.Th., 1980. Environmental Isotopes as Tools in Practical Geohydrology. Groundwater 1980. Geological Society of South Africa, Pretoria.

Vogel, J.C., Fuls, A., Ellis, R.P., 1978. The geographical distribution of Kranz grasses in South Africa. South Africa Journal of Science 74, 209–215.

Vogel, J.C., Kronfeld, J., 1997. Calibration of radiocarbon dates from the Late Pleistocene using U/Th dates on stalagmites. Radiocarbon 39 (1), 27–35.

Von Storch, H., Zwiers, F.W., 1999. Statistical Analysis in Climate Research. Cambridge University Press, Cambridge, 484pp.

Wang, Y.J., Cheng, H., Edwards, R.L., et al., 2001. A high-resolution absolute-dated Late Pleistocene monsoon record from Hulu Cave, China. Science 294 (5550), 2345–2348.

Zhu, J., Wang, S., 2002. Eighty-year oscillation of summer rainfall over North China and East Asian Summer Monsoon. CLIVAR Exchanges 7, 20–23.

Zonneveld, K.A.F., Ganssen, G., Troelstra, S., Versteegh, G.J.M., Visscher, H., 1997. Mechanisms forcing abrupt fluctuations of the Indian Ocean summer monsoon during the last deglaciation. Quaternary Science Reviews 16, 187–201.